Communication: Mapping water collisions for interstellar space conditions

C.-H. Yang,[1,2] G. Sarma,[1,2] J. J. ter Meulen,[2] D. H. Parker,[1,a)] G. C. McBane,[3] L. Wiesenfeld,[4,a)] A. Faure,[4] Y. Scribano,[4,b)] and N. Feautrier[5]
[1]*Department of Molecular and Laser Physics, IMM, Radboud University, Nijmegen, The Netherlands*
[2]*Department of Applied Molecular Physics, IMM, Radboud University, Nijmegen, The Netherlands*
[3]*Department of Chemistry, Grand Valley State University, Allendale, Michigan 49401, USA*
[4]*Laboratoire d'Astrophysique de Grenoble, UMR 5571 CNRS/Université Joseph-Fourier, Grenoble, France*
[5]*LERMA, Observatoire de Paris-Meudon, CNRS UMR 8112, Meudon, France*

(Received 9 March 2010; accepted 24 June 2010; published online 6 October 2010)

We report a joint experimental and theoretical study that directly tests the quality of the potential energy surfaces used to calculate energy changing cross sections of water in collision with helium and molecular hydrogen, at conditions relevant for astrophysics. Fully state-to-state differential cross sections are measured for H_2O-He and H_2O-H_2 collisions at 429 and 575 cm^{-1} collision energy, respectively. We compare these differential cross sections with theoretical ones for H_2O+H_2 derived from state-of-the-art potential energy surfaces [P. Valiron *et al.*, J. Chem. Phys. **129**, 134306 (2008)] and quantum scattering calculations. This detailed comparison forms a stringent test of the validity of astrophysics calculations for energy changing rates in water. The agreement between theory and experiment is striking for most of the state-to-state differential cross sections measured. © *2010 American Institute of Physics*. [doi:10.1063/1.3475517]

Interpretation of the molecular rotational spectra delivered by Earth and space-borne telescopes is a complex process requiring knowledge of molecular state-to-state collisional excitation rates over a broad range of temperatures and transitions. Because these rates for energy changing (inelastic) collisions are not usually known experimentally,[1,2] astronomical models rely predominantly on theoretical estimates that require accurate intermolecular potential energy surfaces (PESs). Water is the most abundant polyatomic molecule in the Galaxy. Detailed knowledge of the energy transfer rates and mechanisms for water is critical in many astrophysical applications, including line transfer, thermal balance of interstellar clouds, and the occurrence of astrophysical masers.[3]

Our work is designed to test the PES describing the interaction of H_2O with H_2 and He, which are the dominant colliders in most astronomical environments. A stringent test of the accuracy of a PES is its ability to predict state-to-state differential cross sections (DCSs), which are sensitive probes of those regions of the interaction potential that govern energy transfer. In media with little ionization, water molecules collide with H_2 molecules in one of the lowest rotational states, or with He atoms, at collision energies in the range from a few cm^{-1} to a few hundreds of cm^{-1}.[3,4] In our laboratory, we collide H_2O with $>90\%$ in its lowest rotational state with H_2 or He at collision energies of 575 and 429 cm^{-1}, respectively.

Previous experiments by Buck and co-workers[5] measured partially state-resolved DCSs for $He+H_2O$ scattering. Nesbitt and co-workers[6] reported state-selective integral cross section measurements for H_2O+argon scattering. Cappelletti and co-workers[7,8] measured total integral cross sections for H_2O+rare gas scattering. Our specific goal here is to determine the *angular distribution* in the center of mass frame of the nascent excited H_2O state flux created by scattering the ground state H_2O by H_2 or He. Such a measurement is now possible using the velocity map imaging (VMI) method.[9,10]

The experimental procedure and VMI apparatus is described in Fig. 1 and is similar to that of Ref. 10. Full details of the apparatus[11] and the nascent water laser ionization detection method[12] will be given in forthcoming publications. In short, molecular beams of water and H_2 or He are crossed at 90°, where H_2O and H_2 are prepared predominately in their lowest possible rotational states. Collisions produce nascent H_2O in higher rotational states. State selective ionization under velocity mapping conditions produces an image of the nascent final state three-dimensional velocity distribution. A typical raw image is shown in Fig. 2(a). Experimental conditions are optimized to minimize the formation of water clusters. Our experiment detects water monomers; if water clusters arise from scattering water, the location and size of the Newton sphere (Fig. 2) will be quite different from that of a monomer collision because of the different kinematics and the dynamics of the cluster dissociation. The images shown in Fig. 2 display no evidence of cluster contributions. We assume that clusters do not affect the results of this study.

In Fig. 2, the rotational quantum states of H_2O are labeled J_{K_a,K_c}, where J is the total rotational angular momentum, and K_a and K_c are projections of J on the a and c rotation axis. The nuclear spin statistics of two identical hydrogen atoms results in two forms of H_2O, *ortho* (K_a+K_c =odd), and *para* (K_a+K_c=even), and two forms of H_2, *para* (J=even) and *ortho* (J=odd). Inelastic collisions conserve

[a)]Authors to whom correspondence should be addressed. Electronic addresses: parker@science.ru.nl and laurent.wiesenfeld@obs.ujf-grenoble.fr.
[b)]Present address: Laboratoire Interdisciplinaire Carnot, UMR 5209 CNRS/Université de Bourgogne, Dijon, France.

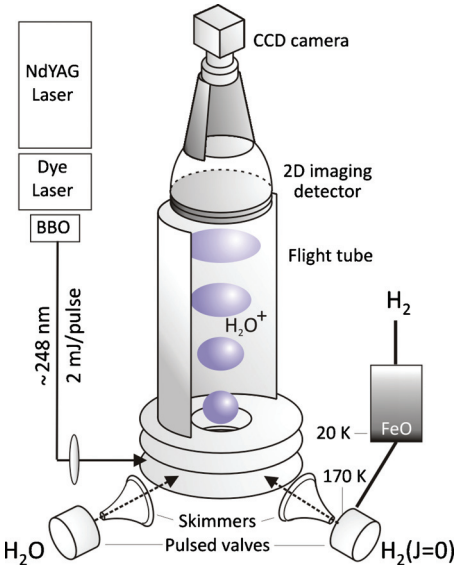

FIG. 1. Schematic of the crossed-beam VMI apparatus. Pulsed molecular beam expansions of pure H_2 or He and H_2O in Ar are skimmed and crossed at 90°. Newly formed rotationally excited H_2O is state selectively ionized by a pulsed laser operating around 248 nm. The H_2O^+ ions are projected by a VMI lens to a two-dimensional imaging detector monitored by a charge coupled device (CCD) camera. Normal H_2 was converted to *para*-H_2 using an iron oxide catalyst at 20 K and was then expanded through a pulsed valve externally cooled by cold N_2 gas to a temperature of 170 K in order to decrease the population of $H_2(J=2)$.

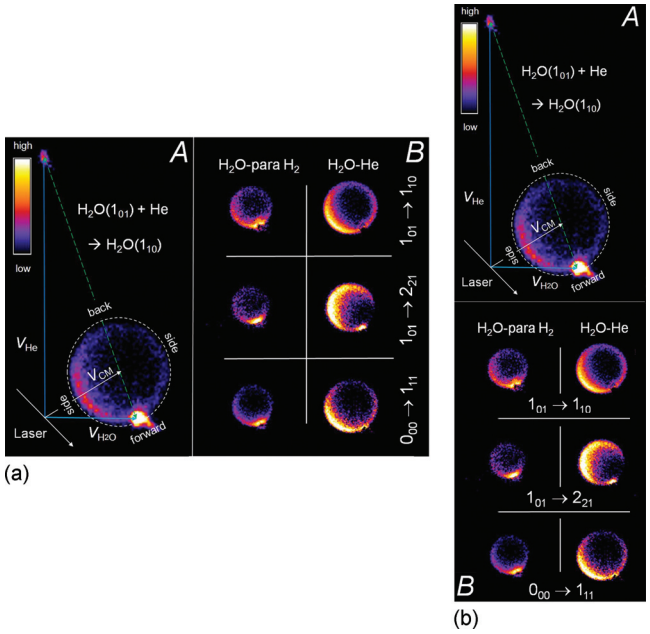

FIG. 2. (a) Raw image of H_2O in the $(J_{K_a,K_c}=1_{10})$ final state created by scattering of $H_2O(1_{01})$ with helium. A color bar on the left side shows the linear intensity scale for the signal. Three signals are seen; a trace amount of water in the He beam (v_{He}, vertical direction), the residual (~5%) population of $H_2O(1_{01})$ in the water beam (v_{H_2O}, horizontal direction), and the two-dimensional projection of the three-dimensional Newton sphere moving at the center of mass velocity (v_{CM}). The dashed circle indicates the size of the Newton sphere for elastic scattering and the directions described as forward, side, and backscattering in the center-of-mass frame (0°, 90°, and 180° in the DCS plotted in Fig. 3). The lower left diagonal arrow shows the propagation direction of the ionization laser beam. (b) Background subtracted images of inelastically scattered H_2O in the indicated final J_{K_a,K_c} state for collisions with *para*-H_2 and He.

ortho-para symmetry.[6]

Images collected with the H_2O and H_2 or He beam separated in time were subtracted from images collected in optimal time overlap for background correction. A set of background-corrected images is shown in Fig. 2(b). These images are *density maps* of nascent H_2O; conversion to the desired *flux map* is carried out using the IMSIM software procedure,[13,14] which reproduces a simulated density image in quantitative agreement with the raw images. The derived flux angular distributions (DCSs, $d\sigma/d\theta$) for the selected images are shown as black lines in the panels of Fig. 3.

An important experimental observation is that for the same final states at nearly the same collision energy, water scatters much more strongly in the forward direction (defined in Fig. 2) due to collisions with H_2 compared to He. Changing the H_2 supersonic beam conditions (using *para*-H_2 versus normal-H_2 and cooling the H_2 nozzle assembly from ~330 to 170 K), we find that the scattering remains strongly in the forward direction. Forward scattering is thus favored for *all* rotational states of H_2. Hence, an important difference between H_2 and He is indicated in our differential measurements, even when scattering is for the most part by *para*-$H_2(J=0)$, which is often assumed to behave similarly to He.[15]

The experimental data are compared here with DCS predictions from a fully quantum analysis using the most recent and advanced PES for the nonreactive systems H_2O+He (Ref. 16) and H_2O+H_2.[17,18] Few such calculations exist in literature.[1,19] For the H_2O+H_2 case, a full nine-dimensional PES (including all inter- and intramolecular degrees of freedom) was obtained from Ref. 18. This nine-dimensional PES was averaged over the vibrational ground state wave functions of H_2O and H_2, yielding a five-dimensional rigid-body PES. This latter PES has been used to calculate many energy changing cross sections and rates relevant for astrophysics,[20–22] making it all the more important to perform the present evaluation. The H_2O-He PES was derived from the PES of Hodges *et al.*[16] using their routines as input to our fitting scheme, which is similar to the original scheme of Green *et al.*[23]

The scattering *S*-matrices needed for computing DCSs for both H_2O-H_2 and H_2O-He were calculated by employing the close coupling formalism implemented in the MOLSCAT program.[24] For H_2 with $J=1,2$, the DCS calculation made use of an algorithm derived from the original DCS formulas.[25] Inelastic cross sections of interest were converged to 1%. For the specific angles 90°, 135°, and 180°, the convergence of DCSs was checked again for a convergence better than 0.5%. The experimental collision energy spread is about ±10%, so we checked the sensitivity of the computed DCS to $E_{collision}$. The sensitivity was marginal, which is expected since the experiments sample transitions between the lowest rotational levels of H_2O, and all scattering resonances for those transitions occur at much lower $E_{collision}$.[26,27] In the case of He, very similar DCS results were obtained in Ref. 5, providing an independent check of our method.

To compare the computed DCS with the experiment for

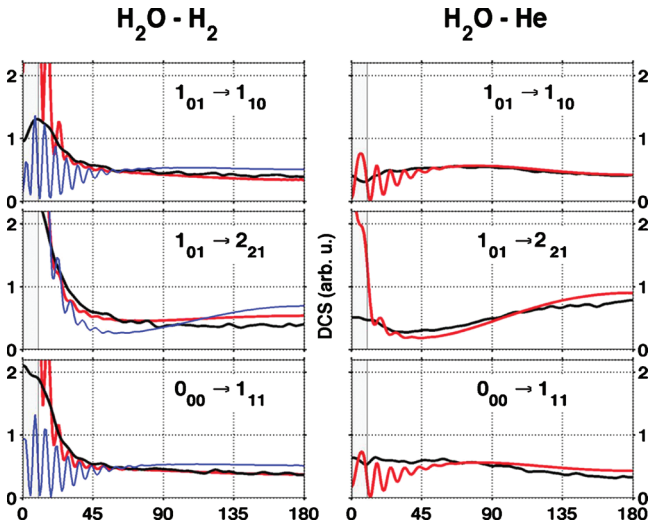

FIG. 3. Experimental and theoretical differential cross sections for H_2O-H_2 inelastic scattering (left column) and H_2O-He inelastic scattering (right column). Black lines (experimental). Red lines, full theoretical DCS calculations. Blue lines, for H_2O-H_2 scattering, theoretical calculations with H_2 in $J=0$ as initial and final states (see text). Scattering angle (deg), *x*-axes; DCS in arbitrary units, all normalized to unity, *y*-axes. Scattering energies: H_2O-H_2, 575 cm^{-1}; H_2O-He, 429 cm^{-1}. Experimental signal in the region of 0°–10° is not reliable due to background subtraction uncertainty.

the H_2O-*para*-H_2 collision (rotational temperature of *para*-$H_2 \sim 220$ K), we averaged the theoretical DCS over a rotational distribution in the H_2 beam of 61% $H_2(J=0)$, 10% $H_2(J=1)$, and 29% $H_2(J=2)$, as measured experimentally using (2+1) Resonance Enhanced Multi-Photon Ionization (REMPI) of H_2 around 200 nm. Collisions resulting in $H_2(J)$ changing cross sections were both measured [using 2+1 REMPI of $H_2(J=1,2)$ at ~200 nm] and calculated to be negligible. Comparisons of the experimental and fully quantum calculated DCSs plotted in Fig. 3 show remarkably good agreement for both the H_2O+He and the H_2O+*para*-H_2 systems. We have not smoothed any possible quantum oscillations appearing in the theoretical DCS. Some remnants of the oscillations averaged over the experimental resolution may be visible at the experimental level.

For the sake of comparisons between He and *para*-H_2 scattering, we also show computed DCSs for scattering between water and *para*-H_2 using the H_2 $J=0,2$ rotor states in the channel basis as before, but considering only $J=0$ initial and final states. In this calculation, the coupled channel propagation used for computation of the *S* matrix elements includes a full description of molecular H_2, including its anisotropy, but the partial wave sum used for construction of the DCS from the *S* matrix elements is identical to that for H_2O-H_2 collisions. The resuts are shown as blue lines in the left panels of Fig. 3. In this case. the DCS structure becomes very different from the results that include an average over the experimental rotational state distribution. The strong forward scattering disappears and the overall structure becomes qualitatively similar to scattering of H_2O by He. Very similar results were obtained when only $J=0$ was included in the H_2 rotor basis, that is, when H_2 was treated as an atom in the scattering calculation. Apparently the most important difference between scattering by He and by H_2 $(J=0)$ is the different shape of the potential; in particular, the well is deeper for H_2. While no attempt is given here to compare absolute values of cross sections, the computed DCSs for He and for H_2 $(J=0 \rightarrow 0)$ show strong similarities at the energies studied, away from the resonance regimes.

H_2O-H_2 scattering is thus quite sensitive to the initial rotational state of the H_2, even though most collisions result in no change in its rotational state. Ignoring this dependence and treating all H_2 molecules as $J=0$ molecules or as atoms can introduce important errors. The common procedure of estimating rates for *para*-H_2 collisions with those from simpler He calculations should thus be applied with caution.

Differences in the scattering of water by *para*-H_2 and normal-H_2 have been found in pressure broadening experiments and simulations at $50<T<200$ K.[28,29] The present experiments, however, did not detect a qualitative change in the DCS changes in H_2 beam conditions. In our experiment, it is not possible to produce a beam of pure *para*-$H_2(J=0)$. Even at the nozzle temperature of 170 K, the expected population ratio of *para*-$H_2(J=0)$ to *para*-$H_2(J=2)$ is still 4.3:1. Replacing normal-H_2 by *para*-H_2 at this temperature in our apparatus produced beams with measured H_2 populations in $J>0$ states of 28%, and the observed images had quite similar angular distributions to those observed under other beam conditions. It is likely that this state distribution was not pure enough to reveal the He-like DCS predicted by the calculation. These experimental indications are qualitative for the present apparatus configuration because the reliability of the signal in the forward scattering region suffers from wide beam angles and background subtraction uncertainty. Improved experiments with more narrow beams and a higher accuracy in the forward scattering region, and more detailed comparisons with scattering by the other rare gases as well as by D_2 (whose spin statistics are inverted with respect to H_2) are under way. Lower collision energies will also be studied using a smaller molecular beam crossing angle.

In summary, experiments are now possible that provide sensitive information in the form of state-to-state differential cross sections for collisions of H_2O with H_2, He, and other species under conditions relevant to those of interstellar space. Although the center-of-mass energy tested here is somewhat higher than the usual energies found in interstellar matter, the shape of the PES has been thoroughly tested, setting great confidence in the calculating scheme that we used to obtain the PES. The measured and calculated properties for the most part agree quite well, giving confidence in the quality of the PESs describing the H_2O-H_2 and H_2O-He interactions. The PESs for H_2O interaction with He and H_2 in general appear to pass the experimental DCS test with flying colors. Our results point out the differences between collisions of water with helium and with cold *para*-H_2, and suggest similarities in the shape of the DCS for all initial $H_2(J)$ states.

Various tests at lower collision energies, including H_2-H_2O cluster spectroscopy, and scattering experiments testing the resonance or elastic regimes should be undertaken in parallel with more global tests such as pressure broadening or virial coefficient measurements. All these tests

comparing theory with experiment help assess the validity of the H_2O-H_2 PES of paramount importance to understanding of the abundance and role of water in the interstellar matter.

The authors in Nijmegen acknowledge Leander Gerritsen for expert technical assistance. Most of this work, in Nijmegen and in Grenoble, was supported by the European FP6 program "Molecular Universe."

[1] M. L. Costen, S. Marinakis, and K. G. McKendrick, Chem. Soc. Rev. **37**, 732 (2008).
[2] P. W. Barnes, I. R. Sims, and I. W. M. Smith, J. Chem. Phys. **120**, 5592 (2004).
[3] M. Elitzur, *Astronomical Masers* (Springer, New York, 1992).
[4] B. Lefloch, J. Cernicharo, B. Reipurth, J. R. Pardo, and R. Neri, Astrophys. J. **658**, 498 (2007).
[5] J. Brudermann, C. Steinbach, U. Buck, K. Patkowski, and R. Moszynski, J. Chem. Phys. **117**, 11166 (2002).
[6] W. B. Chapman, A. Kulcke, B. W. Blackmon, and D. J. Nesbitt, J. Chem. Phys. **110**, 8543 (1999).
[7] D. Cappelletti, V. Aquilanti, E. Cornicchi, M. Moix Teixidor, and F. Pirani, J. Chem. Phys. **123**, 024302 (2005).
[8] V. Aquilanti, E. Cornicchi, M. M. Teixidor, N. Saendig, F. Pirani, and D. Cappelletti, Angew. Chem., Int. Ed. **44**, 2356 (2005).
[9] A. T. J. B. Eppink and D. H. Parker, Rev. Sci. Instrum. **68**, 3477 (1997).
[10] K. T. Lorenz, D. W. Chandler, J. W. Barr, W. Chen, G. L. Barnes, and J. I. Cline, Science **293**, 2063 (2001); H. Kohguchi, T. Suzuki, and M. H. Alexander, *ibid.* **294**, 832 (2001).
[11] C.-H. Yang, G. Sarma, J. J. ter Meulen, D. H. Parker, G. C. McBane, and L. Wiesenfeld (unpublished).
[12] C.-H. Yang, J. J. ter Meulen, D. H. Parker, and C. M. Western, "REMPI spectroscopy and predissociation of the $C^1B_1(v=0)$ rotational levels of H_2O, HOD, and D_2O," Phys. Chem. Chem. Phys. (submitted).
[13] G. C. McBane, "IMSIM" program, version 2, available at http://faculty.gvsu.edu/mcbaneg/.
[14] K. T. Lorenz, D. W. Chandler, and G. C. McBane, J. Phys. Chem. A **106**, 1144 (2002).
[15] N. Troscompt, A. Faure, M. Wiesenfeld, C. Ceccaelli, and P. Valiron, Astron. Astrophys. **493**, 687 (2009).
[16] M. P. Hodges, R. J. Wheatley, and A. H. Harvey, J. Chem. Phys. **116**, 1397 (2002).
[17] A. Faure, P Valiron, M. Wernli, L. Wiesenfeld, C. Riste, J. Noga, and J. Tennyson, J. Chem. Phys. **122**, 221102 (2005).
[18] P. Valiron, M. Wernli, A. Faure, L. Wiesenfeld, C. Rist, S. Kedžuch, and J. Noga, J. Chem. Phys. **129**, 134306 (2008).
[19] B. Yang and P. C. Stancil, J. Chem. Phys. **126**, 154306 (2007).
[20] M. L. Dubernet, M.-L. Dubernet, F. Daniel, A. Grosjean, A. Faure, P. Valiron, M. Wernli, L. Wiesenfeld, C. Rist, J. Noga, and J. Tennyson, Astron. Astrophys. **323**, 460 (2006).
[21] A. Faure, N. Crimier, C. Ceccarelli, P. Valiron, L. Wiesenfeld, and M. L. Dubernet, Astron. Astrophys. **472**, 1029 (2007).
[22] M. L. Dubernet, F. Daniel, F. A. Grosjean, and C. Y. Lin, Astron. Astrophys. **497**, 911 (2009).
[23] T. R. Phillips, S. Maluendes, and S. Green, J. Chem. Phys. **102**, 6024 (1995).
[24] J. M. Hutson and S. Green, MOLSCAT computer code, version 14 (1994), distributed by Collaborative Computational Project No. 6 of the Engineering and Physical Sciences Research Council (U.K.).
[25] A. R. Edmonds, *Angular Momentum in Quantum Mechanics*, 4th ed. (Princeton University Press, Princeton, NJ, 1996).
[26] See Fig. 1, A. Grosjean, M.-L. Dubernet, and C. Ceccarelli, Astron. Astrophys. **408**, 1197 (2003).
[27] See Fig. 2, M.-L. Dubernet and A. Grosjean, Astron. Astrophys. **390**, 793 (2002).
[28] M. J. Dick, B. J. Drouin, and J. C. Pearson, J. Quant. Spectrosc. Radiat. Transf. **110**, 619 (2009).
[29] L. Wiesenfeld and A. Faure, "*Ab initio* computation of the broadening of water rotational lines by molecular hydrogen," Phys. Rev. A (submitted).